Journal of Physical Science, Vol. 33(1), 29–49, 2022

Study of Physico-Chemical Properties and Growth Dimension Augmentation of Barium Succinate Single Crystals Grown by Slow Evaporation Technique

Christy D. S.[1*], Sahaya Shajan X.[2] and Mahadevan C. K.[3]

[1]Post Graduate and Research Department of Physics, St. John's College, Palayamkottai, Tirunelveli 627 002, Tamil Nadu, India
[2]Centre for scientific and applied research, PSN College of Engineering and Technology, Tirunelveli 627 152, Tamil Nadu, India
[3]CSIR Emeritus Scientist, Department of Physics, Bharathidasan University, Tiruchirappalli 620024, Tamil Nadu, India

[*]Corresponding author e-mail: balasam50@gmail.com

Published online: 25 April 2022

To cite this article: Christy, D. S., Sahaya, S. X. & Mahadevan, C. K. (2022). Study of physico-chemical properties and growth dimension augmentation of barium succinate single crystals grown by slow evaporation technique. *J. Phys. Sci.*, 33(1), 29–49. https://doi.org/10.21315/jps2022.33.1.3

To link to this article: https://doi.org/10.21315/jps2022.33.1.3

ABSTRACT: *Slow evaporation method was adopted to grow barium succinate (BS) single crystals for the first time and diamond shape crystals were successfully synthesised with dimension 14 mm³ × 17 mm³ × 4 mm³. Single crystal x-ray diffraction studies show that the crystal system is monoclinic. Powder x-ray diffraction studies confirmed the crystallinity of the grown BS crystal. From energy dispersive x-ray spectroscopy (EDS) analysis the presence of barium metal was confirmed. The functional group of the BS crystal was confirmed from fourier transform infrared (FTIR) spectrum. The crystals were found to be hydrated and thermally stable up to 150°C. BS crystal possesses good transmittance in the wavelength range 250 nm–1200 nm and it is non-linear optical (NLO) active material. The BS crystals have mechanical softness and normal dielectric behaviour.*

Keywords: x-ray diffraction, crystal growth from solution, barium compounds, mechanical hardness, dielectric materials, NLO crystal

1. INTRODUCTION

Crystal growth is the most important field of research and technology. Fabrication of compounds based on metal-organic frameworks has become an important area of research in crystal engineering and materials.[1] Metal-organic framework crystals are currently receiving a great deal of attention due to the rapid development of laser diodes and significant regards to their fascinating structures and potential applications in hydrogen storage, electrical and magnetic properties, nonlinear optical properties, luminescence and use as catalysts.[2] Compared with the extensively investigated transition metal coordination polymers, relatively a small number of alkaline earth coordination polymers are reported in literature. A great deal of work has been reported on the growth and characterisation of metal-organic frameworks of transition metals with dicarboxylic acids such as tartaric, oxalic, and malonic acids but less with succinates.[2] However, metal succinate frameworks have increased the range of possible applications by their physical properties.[2–7]

Metal complexes of single crystals are better alternatives for potassium di-hydrogen phosphate (KDP) crystals in the field of high-power frequency conversion, frequency doubling and laser fusion experiments due to their high values of laser damage threshold and mechanical strength. This is because, metal complexes of barium which have low UV cut-off wavelengths. Barium is a metal alkaline earth metal. In vacuum tubes, high temperature superconductors, it can be used.[8]

Studies on barium succinate single crystals grown in gel medium have been reported by Binitha and Pradyuman.[4] They obtained barium succinate crystals up to a maximum size of 3 mm^3 × 2 mm^3 × 0.2 mm^3 grown by the gel method. They found that the crystal structure is tetragonal with cell parameters: a = 7.58 Å and c = 10.24 Å. This is in agreement with that available in the ICDD file card no. 00-0050-2415 for the barium succinate (BS) crystal.

The bid assignment for crystal growers is to grow bulk size crystals with the measure of efficiency at the lofty level and hence realise their utilisation for various fields. After undergoing so many experimental variations and rectifications, the process of slow evaporation solution growth technique yields good quality unidirectional and bulk crystals for a variety of utilisations. Hence in order to get large size crystals, seeded free evaporation or slow cooling method is normally adopted. The seed crystals can be grown by the free (slow or solvent) evaporation method.

In the present investigation, we have attempted to grow BS single crystals by the solvent evaporation method for the first time and characterise the grown crystals. Moreover, we have considered barium carbonate ($BaCO_3$) instead of barium chloride ($BaCl_2$) as one of the precursors. The structural, thermal, optical, mechanical and electrical characteristics have been reported in this paper.

2. EXPERIMENTAL

2.1 Materials Used

$BaCO_3$ (RANKEM 97%) and high purity succinic acid (HIMEDIA 99%) along with de-ionised water were used as the required materials for the growth of single crystals in the present study.

2.2 Crystal Growth

In a particular molar concentration succinic acid and $BaCO_3$ were taken and dissolved in de-ionised water of resistivity 18.2 MΩcm. The BS crystals were prepared according to the reaction:

$$BaCO_3 + C_4H_6O_4 \text{ (in aqueous solution)} \rightarrow BaC_4H_4O_4 \cdot nH_2O + H_2CO_3$$

The synthesised crystals were further purified by repeated recrystallisation process. Good quality single crystals (seed crystals) with diamond shape and size up to 4 mm^3 × 3 mm^3 × 2 mm^3 were harvested within 25 days. The crystal holder was connected to microcontroller, which is used to rotate the crystalliser clockwise and anticlockwise. This bidirectional rotation was used to make the solution homogeneous and avoid inclusions in the crystal. A 500 ml saturated solution was prepared and filtered using a Whatman filter paper. A good seed crystal was selected from the crystals grown by the slow evaporation method and mounted on the crystal holder. Crystal holder was made up of acrylic used to stir the saturated solution very well and make the solution more stable. A bulk crystal of BS was harvested after 65 days, and the size of the crystal is 14 mm^3 × 17 mm^3 × 4 mm^3. A photograph of the bulk BS single crystal grown is shown in Figure 1. The crystal is found to be considerably stable in the normal atmosphere.

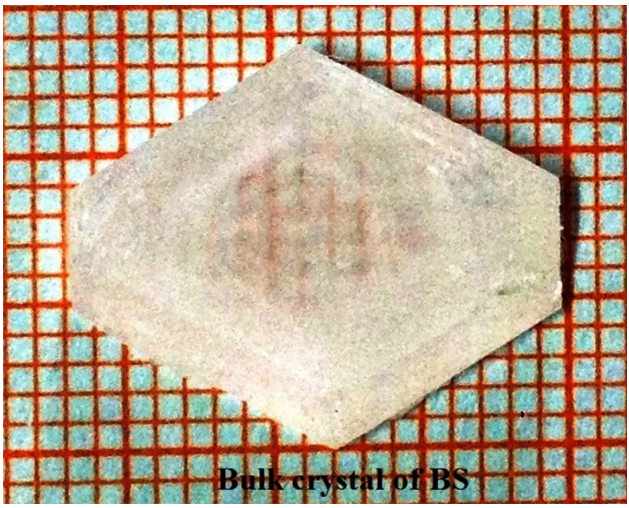

Figure 1: A Photograph of the bulk BS crystal grown.

2.3 Material Characterisation

Good crystals without any visible defect have been selected and subjected to various measurements in order to characterise them chemically, structurally, thermally, optically, mechanically and electrically by the available standard methods.

The basic structural and chemical features of the grown BS crystals were examined by single crystal x-ray diffraction (SXRD) analysis to determine the cell parameters and morphology of the crystal using a (BRUKER X8/America) highly versatile 4 circle kappa goniometer with M_OK_α radiation (λ = 0.71073 Å) and APEXII detector. To understand the crystalline nature of the BS crystal grown, powder x-ray diffraction (PXRD) analysis was carried out using an (XPERT-PRO/Netherlands) PANanalytical diffractometer having CuK_α radiation (λ=1.54014 Å) over the (angular) 2θ range 10°–80°.

To analyse the vibrational modes of the BS single crystals, fourier transform infrared (FTIR) spectral measurements was carried out using a (JASCO FTIR-4100/Japan) spectrometer in the wave number range 550 cm^{-1}–4000 cm^{-1} by attenuated total reflection (ATR) technique. Energy dispersive x-ray spectroscopy (EDS) was used to examine the metal atom content present in the grown crystals using a (JEOL model 9JED 2300/Japan).

Differential thermogravimetric (DTG) and thermogravimetric analyses (TGA) give information regarding water of crystallisation, different stages of decomposition and phase transition of the crystal system. TGA/DTG was carried out for the grown crystal BS in the temperature range 38°C–700°C in a nitrogen atmosphere with a heating rate of 10°C/min using a (PERKIN ELMER DIAMOND TG/DTG/UK) analyser.

An optical property of the grown BS crystal was studied by a SHIMADZU (DRS UV – 2600/Japan) spectrophotometer in the wavelength range 200 nm–1200 nm with the sample thickness 1.7 mm. Adopting Kurtz and Perry powder technique, the second harmonic generation (SHG) efficiency of the powdered sample of BS single crystal was studied using a Q-switched (Nd: YAG laser/US) delivering energy of 1 mJ/pulse at 1064 nm with a repetition rate of 10 Hz and pulse width of 10 ns.[9]

The mechanical property of the grown BS crystal was examined by Vicker's micro hardness measurement using a SHIMAZDU (HMV - 2T/Japan) hardness tester with diamond indenter. The diagonal length of the indentations was measured by keeping a constant indentation time of 5 s and applied by various loads (P) ranging from 25 g–100 g. The dielectric properties of the grown BS single crystal were investigated by a (HIOKI IM 3523/China) LCR meter to an accuracy of ±2% at various temperatures ranging from 35°C–145°C and with various frequencies ranging from 100 Hz–200 kHz.

3. RESULTS AND DISCUSSION

3.1 PXRD Analysis

The PXRD pattern observed in the present study is shown in Figure 2. It is observed that the relative intensities (at 2θ values) have been changed and a slight shift in the peak position (2θ values) was observed when compared to the reported data. It may be due to the precursors used as well as the method of crystal growth. The prominent well-resolved sharp and strong peaks at specific 2θ values reveal the good crystallinity of the grown crystal.

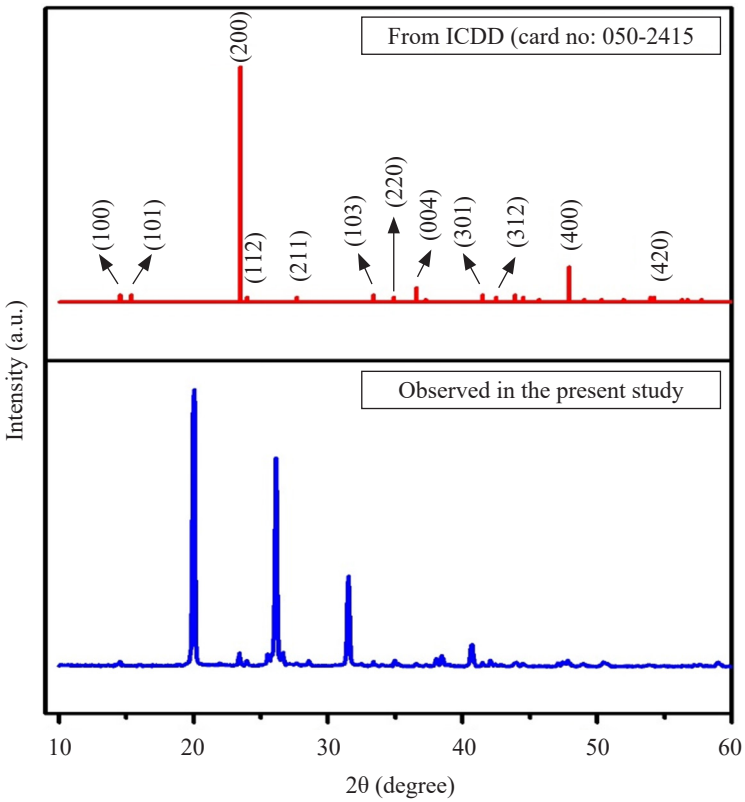

Figure 2: The PXRD pattern observed for the BS crystal grown in the present study compared to that available in ICDDfile.

3.2 SXRD Analysis

The lattice parameters obtained through SXRD analysis are; a = 5.20 Å, b = 9.02 Å and c = 5.60 Å; α = γ = 90° and β = 91.16°; and the volume of the unit cell is found to be 263 $Å^3$. Hence, the result shows that BS crystal belongs to the monoclinic crystal system. The cell parameters obtained in the present study are compared with those reported for BS crystal by earlier authors in Table 1. It can be noted that there is a change in the lattice parameters and crystal system with those reported in the literature. This is because of the presence of water molecule and the change of precursor. The very interesting aspects of metal-organic frame works of transition metals with succinic acid depend on the presence and absence of water molecules.[2–7]

Table 1: The lattice parameters obtained (through SXRD analysis) for the BS crystal grown.

Lattice parameter	From ICDD (card no:050-2415)	Observed in the present study
a (Å)	7.60	5.20
b (Å)	7.60	9.02
c (Å)	10.29	5.60
α (°)	90	90
β (°)	90	91.16
γ (°)	90	90
Volume (Å^3)	594	263
Lattice system	Tetragonal	Monoclinic P

The consequent variation in the crystal structure produces variation in the number of hydrogen bonds in the crystal; hence the number of water molecules is varied. These are all the reasons for change in the system and unit cell parameter values.

3.3 FTIR Analysis

The FTIR analysis of BS crystal was carried out by the ATR method and the recorded spectrum is shown in Figure 3.

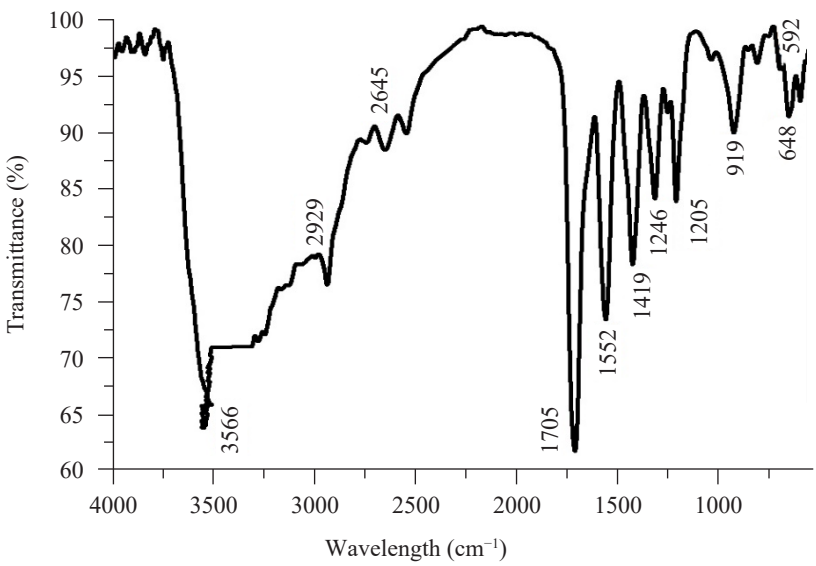

Figure 3: The FTIR spectrum observed for the BS crystal grown.

This confirms the presence of functional groups (assignments given in Table 2) and the coordination ligand to metal ions. In the high frequency region, the broad peak positions between 3600 cm^{-1} and 2750 cm^{-1} which corresponds to the stretching of O-H group.

Table 2: The assignments (through FTIR spectral analysis) of functional groups present in the BS crystal grown.

BS (cm^{-1})	Assignment
3566	H bonded O-H group
2929	ν_sC-H
1705	ν_s COO^-
1552	ν_{as} COO^-
1419	β C-H
1246	$\rho_t(CH_2)$
1205	β C-O-H
919	ν_s C-C
648	ν Metal-O
592	ν Metal-O

Note: ν_s = Symmetric stretching; ν_{as}= Asymmetric stretching; β = In plane bending; ρ_t = Twisting mode; S = Scissoring; δ = Deformation; ω = Wagging / Out of plane bending; ν = Stretching

Hence the BS crystal possesses water molecules. But the earlier authors show no significant peak related to the presence of water molecules. The peaks at 1704 cm^{-1} and 1552 cm^{-1} correspond to the stretching and asymmetric stretching respectively of carboxylate salts (COO^-). The peaks at 1419 cm^{-1}, 647 cm^{-1}, and 919 cm^{-1} correspond respectively to C-H bending, C-H stretching and C-C symmetric stretching. The peak observed below 550 cm^{-1} reveals the coordinate interaction with metal ion which confirms the presence of barium coordinated with oxygen. Hence, in the present study, all the required functional groups could be confirmed by the FTIR analysis.

3.4 EDS Analysis

The technique used to confirm the presence of various elements in the crystal material is the EDS analysis. It is associated with an electron microscope to characterise the material.[10] The qualitative and quantitative determination of the elements present in the sample was obtained by a spectrum consists of energy versus relative counts detected by x-rays. This method can be used to detect the elements which have atomic number more than five. The atomic and weight percentages of the elements (other than the hydrogen) present in the BS crystal grown are given in Table 3.

Table 3: The atomic and weight percentages (obtained through EDS spectrum) of the elements (other than the hydrogen) present in the BS crystal grown.

Element	Weight %	Atomic %
C	55.27	51.63
O	12.85	14.25
Ba	31.88	34.12
Total	100	100

Note: C = Carbon; O = Oxygen; Ba = Barium

The presence of barium in the BS crystal is confirmed by EDS analysis and the barium incorporated into the crystal matrix can be clearly seen in Figure 4.

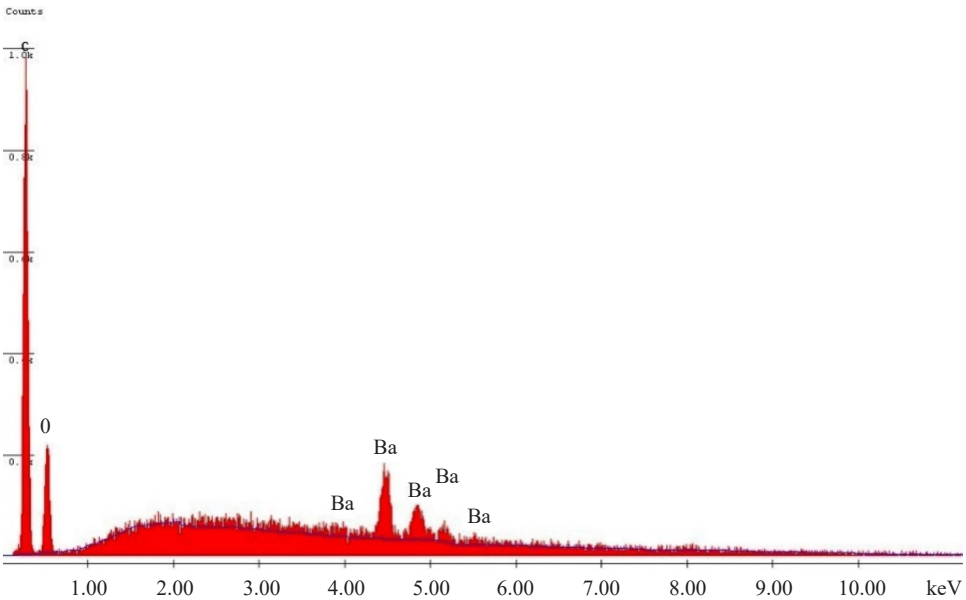

Figure 4: The EDS spectrum observed for the BS crystal grown.

3.5 TGA/DTG Analysis

TGA and DTG analyses give information regarding phase transition, water of crystallisation and different stages of decomposition of the crystal. TGA/DTG curves (patterns) obtained for the BS crystal grown are presented in Figure 5. There is no significant weight loss observed before its decomposition. The BS crystal is thermally stable at least up to 150°C. After that the BS crystal exhibits two stages of decomposition.

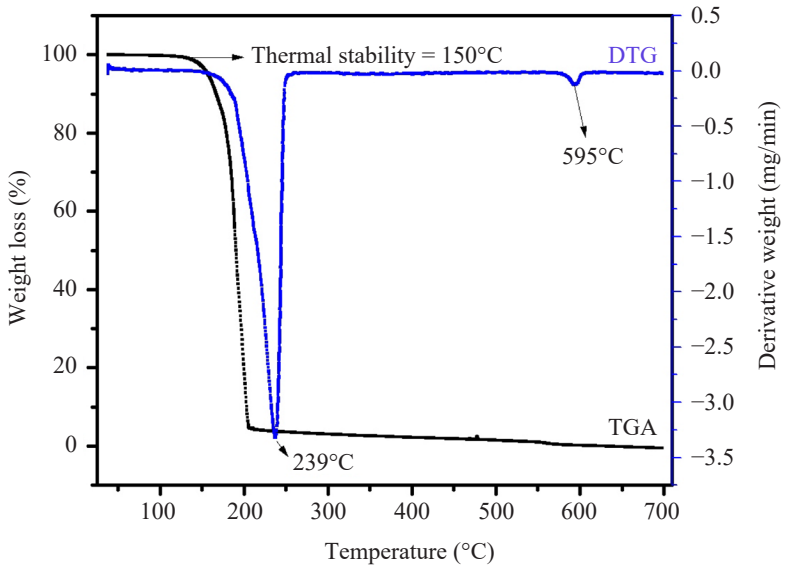

Figure 5: The TGA/DTG patterns observed for the BS crystal grown.

The first one is sharp and the second one is diffuse. The first sharp weight loss ranges from 150°C–206°C. Major weight loss of 92% was observed which indicates that major portion of the compound (as $C_2H_3COOH+CO+Urea+0.8H_2O$) was removed by this decomposition leading to the formation of barium oxide. The FTIR spectral and TGA indicate the presence of about 0.8 (not full) water molecules in the title compound.

The decomposition stages can be represented as:

$$Ba(C_2H_2O_2)_2.0.8H_2O \xrightarrow{(-C_2H_3COOH + CO + Urea + 0.8H_2O)} BaO \xrightarrow{-(BaO)} \text{Trace amount of Ba}$$

Stage I **Stage II**

The second weight loss starts from 475°C–611°C decomposing the barium oxide leading to Ba metal (trace amount) formation. It was verified by heating the BS crystal from 160°C–240°C. When the temperature reaches 210°C, the compound degraded and the colour changed. The BS single crystal is found to be thermally stable at least up to 150°C.

3.6 UV-Vis-NIR Spectral Analysis

In optoelectronic device preparation, single crystals with ample optically transparent (window) wavelength range perform a very fascinating role.

Optically polished single crystal of thickness 3 mm was used for this study. The UV-Vis-NIR transmittance spectrum of BS single crystal was recorded in the wavelength range 200 nm–1200 nm and it is shown in Figure 6.

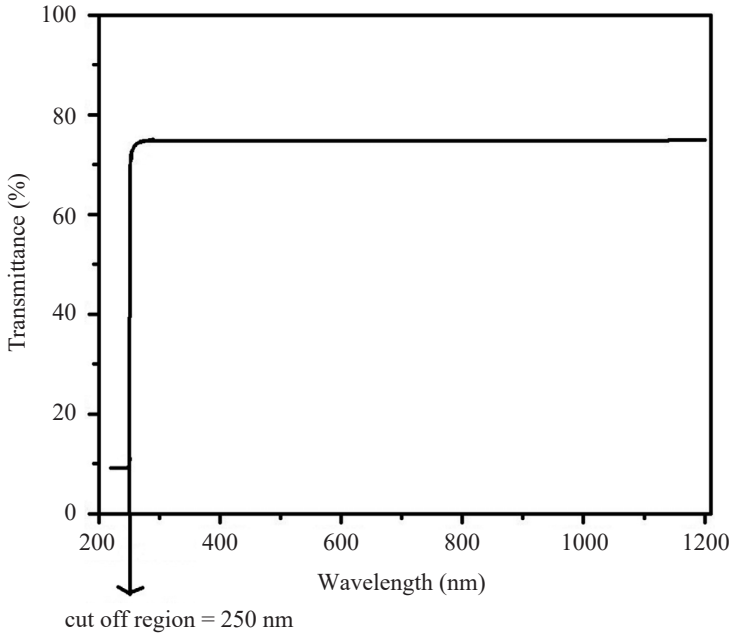

Figure 6: The UV-Vis-NIR spectrum observed for the BS crystal grown.

The grown crystal has 74% transmittance in the entire visible region. It can be noted from Figure 6 that the BS crystal has a lower cut off wavelength at 250 nm, that can be attributed to the electronic transitions in the charge transfer axis. Absence of absorbance in the region between 250 nm–1200 nm is a fundamental claim of the NLO materials. Hence, the crystal can be used as a sensor material for UV-Vis-NIR regions.

3.7 Powder SHG Efficiency

The SHG efficiency of the grown BS crystal was tested by Kurtz and Perry technique and the efficiency of the sample was compared with microcrystalline powder of KDP as the reference material.[9] The SHG efficiency of the output pulse measures for BS is 62 mV and its SHG efficiency is 0.67 times that of KDP. The reported BS single crystal possesses centrosymmetric crystal structure, and, as per the theory, it is not expected to exhibit SHG property. High SHG is normally related with favourable molecular alignment facilitating nonlinearity.[10] The SHG property exhibited by the BS crystal can be explained

as it may be due to the presence of water molecule (possibly) in the centre of inversion symmetry or due to π electron cloud movement from the donor to acceptor molecules or the local noncentrosymmetry caused by defects.[11]

3.8 Mechanical Properties

To understand the mechanical properties of the crystal, the well-known simple and non-destructive testing is the micro hardness measurement. Knowing the mechanical strength of the grown crystal is very important because it plays a pivotal role in device application. The strength and plasticity of any material can be understood by this physical characteristic (hardness property). The hardness of the crystal also depends on the type of chemical bonding, presence of precursors and nature of the material. Hardness is defined as resistance offered to the motion of dislocations, as the ability of a crystal to resist a structural breakdown under applied stress.[12,13] Vickers hardness is one of the important deciding factors for selecting (cutting, grinding, and polishing) bulk crystal in fabrication of devices based on crystal.[14] Microhardness measurement on BS single crystal using the conventional pyramidal diamond indenter will be influenced by the basic anisotropic properties of the crystal. The dimensions of both diagonals of an indentation were measured and the average diagonal d was calculated from all diagonals measured for a particular load P.

The hardness of the crystal was calculated using the relation: kg

$$H_V = 1.8544 \times \left(\frac{P}{d^2} \right) \text{kg/mm}^2 \tag{1}$$

Vickers hardness number increases with the increase in load shown in Figure 7(a) and this is called reverse indentation size effect (RISE). The reason for higher hardness values for higher loads can be understood as due to low resistance to the flow of dislocations. The other reason for this can be the soft crystal surface.

The work hardening coefficient n is the measure of the strength of materials. According to Meyer's law the relationship between load and size of the indentation is given by:

$$P = k_1 d^n \tag{2}$$

Here P is the load applied, d is the diagonal length of impression, k_1 is a constant and n is the Meyer's index. Plot between log P and log d drawn is shown in Figure 7(b) and found to be nearly linear obeying the Meyer's law.

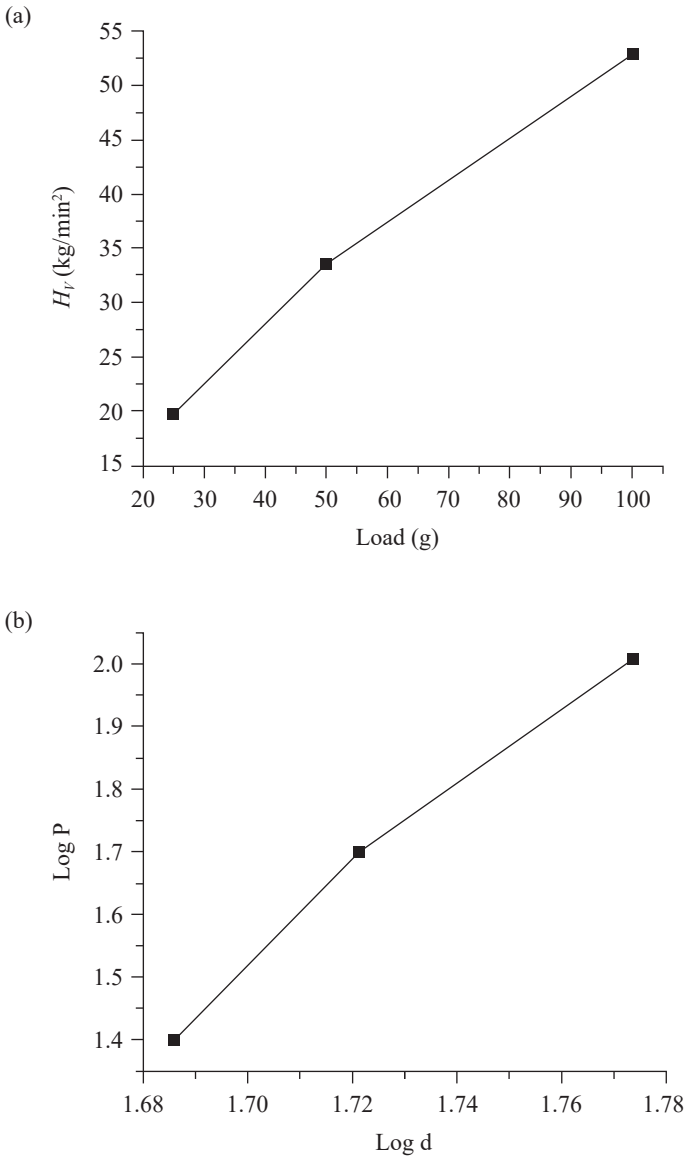

Figure 7: The hardness measurement results obtained for the BS crystal grown: (a)The hardness behaviour, and (b) Plot between log P and log d.

Onitsch and Hanneman had shown that the value of n comes out to be 1–1.6 for hard materials and more than 1.6 for soft ones.[15] The n value is found to be 5.86 in the present investigation. Thus, the BS crystal under investigation belongs to soft material category.

3.9 Dielectric Properties

The dielectric measurements were carried out on the grown BS single crystal with respect to the temperature and frequency. The changes in dielectric constant, dielectric loss factor and AC conductivity versus frequency and temperature observed in the present study are shown in Figures 8, 9 and 10. The dielectric loss was directly measured and dielectric constant and AC conductivity were estimated using the relations:

$$\varepsilon_r = \frac{Cd}{\varepsilon_0 A} \tag{3}$$

$$\sigma_{ac} = \varepsilon_0 \varepsilon_r \omega \tan \delta \tag{4}$$

Here, C is the measured capacitance, d is the thickness of the crystal, A is the area of cross section of crystal touching the parallel electrodes, ω (=$2\pi f$) is the angular frequency and ε_0 is the permittivity of free space. The A and d were measured using a travelling microscope to an accuracy of ± 0.001 cm.

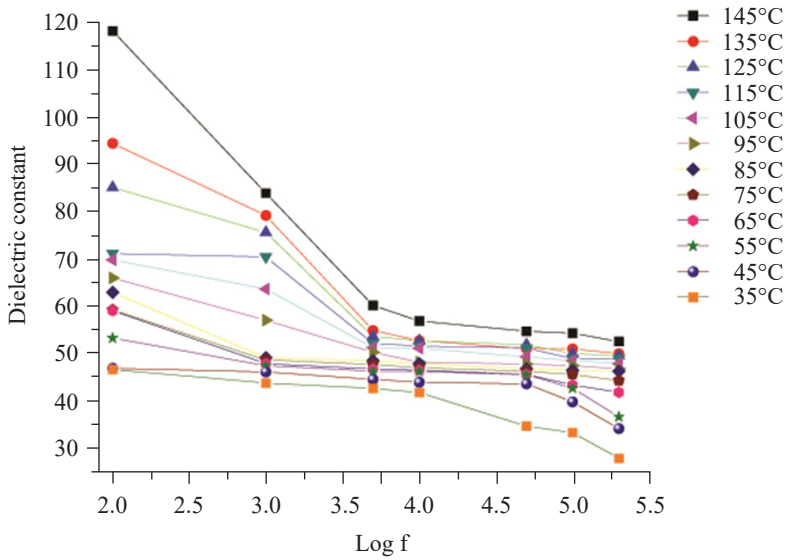

Figure 8: Variation of dielectric constants(ε_r) with frequency at different temperatures observed for the BS crystal grown.

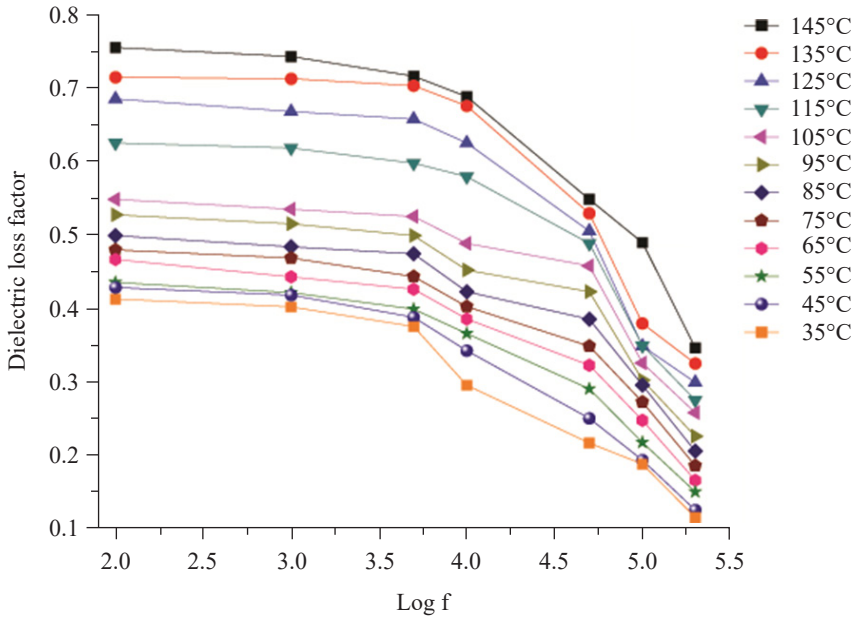

Figure 9: Variation of dielectric loss factor (tan δ) with frequency at different temperatures observed for the BS crystal grown.

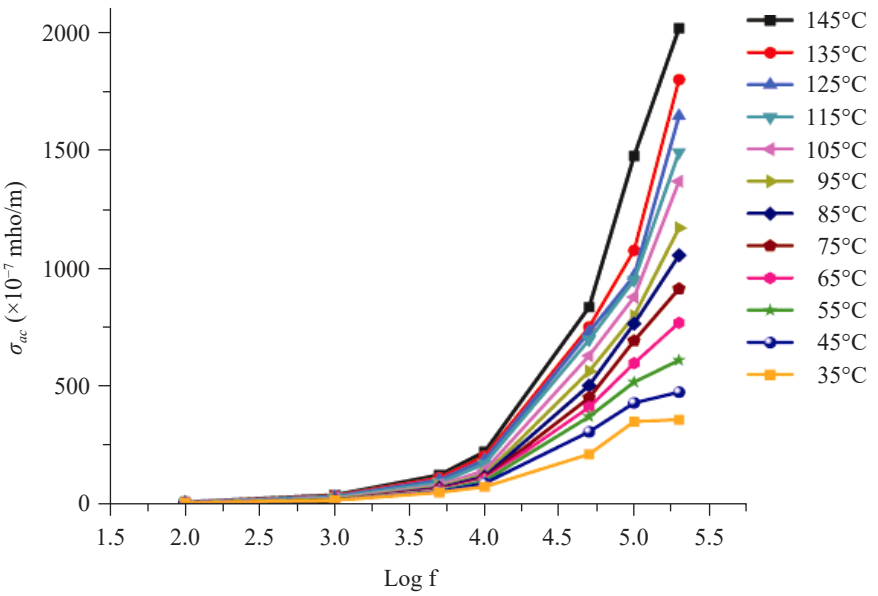

Figure 10: Variation of AC electrical conductivity (σ_{ac}) with frequency at different temperatures observed for the BS crystal grown.

All the three dielectric parameters considered are found to increase with the increase in temperature. Also, when the frequency increases, the ε_r and tan δ values decrease whereas the σ_{ac} value increases. This result indicates that the BS crystal exhibit a normal dielectric behaviour. Dielectric constant of the material is due to electronic, ionic, orientation and space charge polarisations. At low frequencies space charge polarisation is more predominant and hence dielectric constant increases abnormally. As the frequency increases, space charge cannot sustain and comply with the external field and hence polarisation decreases, giving rise to diminishing values of dielectric constant. The low values of dielectric constant at high frequencies are important for the materials in the construction of photonic devices.

The dielectric losses (or dissipation factors) are associated with imperfections in the crystal such as impurities, micro structural defects, porosity, micro cracks and random crystallite orientation. The dielectric loss decreases with the increasing frequency and increases with the increasing temperature. It accounts for good chemical homogeneity of the grown crystal with lesser defects and this parameter is important for materials in the fabrication of photonic and electro optic devices. An essential property of NLO material is its ability to support an electrostatic field while dissipating minimal energy (the lower dielectric loss) in the form of heat.[16] The tan δ values observed for the BS crystal grown in the present study are sufficiently small so that the crystal can be expected to be useful for photonic and electro optic devices.

The imperfection and impurities present in a dielectric material are expected to create potential barriers which limit the transport of charge carriers. As BS crystal grown in the present study is hydrogen bonded dielectric crystal, large amount of proton transport (leading to ionic polarisation) is expected. Also, there is a possibility of weakening the hydrogen bonding system due to rotation of the hydroxyl ions in water molecules when the temperature increases. This is expected to generate vacant hydrogen bonds (L-defects) at higher temperatures. The electrical conductivity of hydrogen bonded crystals can be understood as due to the protonic transport within the framework of hydrogen bonds.[17–19] Moreover, this proton transport depends on the creation of L-defects. The electrical conduction in BS crystal grown in the present study can also be considered as protonic which can be mainly due to the water molecules and succinate ions.

Moreover, the increase of electrical conductivity with the increase in temperature can be explained as due to the temperature dependence of the proton transport. In addition, the electrical conductivity is found to increase smoothly in the

temperature range considered in the present study. The AC electrical conductivity values are found to be fitted into the Arrhenius equation for electrical conductivity:

$$\sigma_{ac} = \sigma_0 \exp[-E_{ac}/kT] \tag{5}$$

Here, σ_0 is a constant depending on the material, E_{ac} is the AC activation energy, k is the Boltzmann constant and T is the absolute temperature. The plots made between $1000/T$ and ln σ_{ac} values (not shown here) gave nearly straight line plots and the slopes of the best fitted straight lines are equal to E_{ac}/kt values, from which the AC activation energies (E_{ac} = −slope × k × 1000) in (eV) were estimated.

The AC power law is related as:

$$\sigma_{ac} = B\omega^m \tag{6}$$

Here, B and m are constants depending on the temperature and material. The B value has the electrical conductivity unit and m is dimensionless. The ln σ_{ac} versus ln ω plots were made according to AC power law and are shown in Figure 11. The plots are found to be nearly linear obeying the power law. From the best fitted lines, the m and B values were estimated. The m values lie in the range 0.78–0.86.

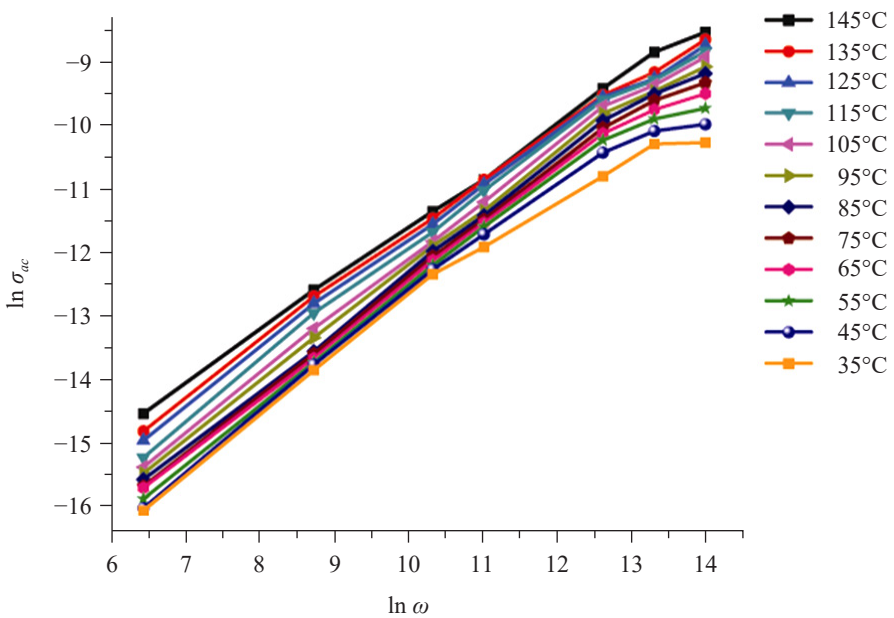

Figure 11: The plots between ln σ_{ac} and ln ω obtained for the BS crystal grown.

In order to verify that the *B* values are DC conductivities, DC electrical conductivity measurement has been carried out in the temperature range 35°C–145°C by using the conventional two-probe method. The measured DC conductivity (σ_{dc}) and *B* (determined using AC power law relation) values are shown in Figure 12.

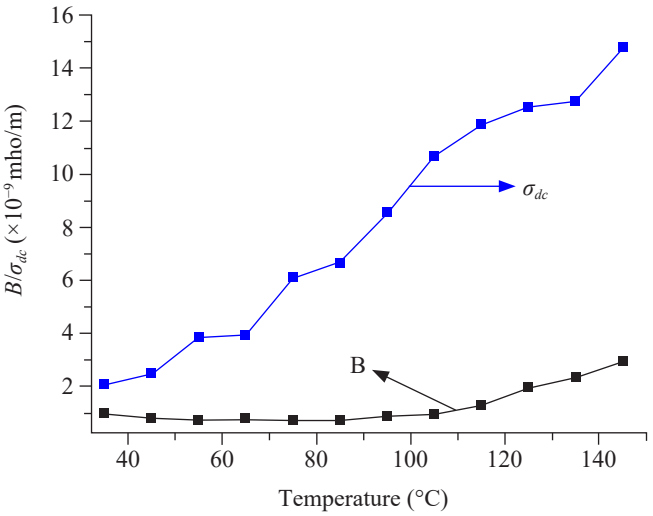

Figure 12: The temperature dependence of B/σ_{dc} obtained for the BS crystal grown.

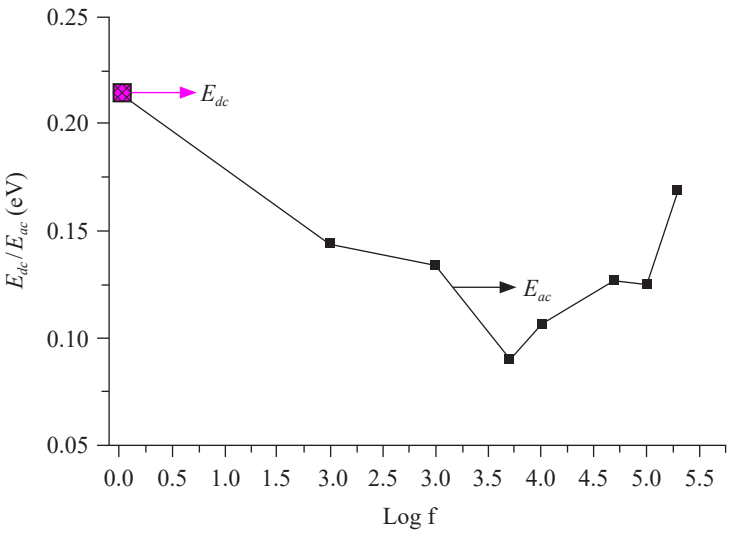

Figure 13: The AC and DC activation energies (E_{ac}/E_{dc}) obtained for the BS crystal grown.

Thus, the results of electrical measurements made in the present study follow the AC Power law. As the measured σ_{dc} values were found to obey the Arrhenius relation, the DC activation energies (E_{dc}) were also determined in a similar way followed for the E_{ac} determination. The calculated values of E_{ac} and E_{dc} are shown in Figure 13. The lower E_{ac} and E_{dc} values obtained indicate that the material considered possesses ionic conductivity.[20–23] Also, it indicates the presence of oxygen vacancies which may lead to L-defects.

4. CONCLUSION

Good quality and large size BS single crystals could be grown successfully by the seeded slow evaporation solution technique. The SXDR analysis revealed the monoclinic structure. The PXRD study enumerated that the structural perfection of the BS crystal is good. The presence of all the functional groups was confirmed by FTIR spectral analysis. EDS spectral analysis confirmed the presence of metal ions. The BS single crystal is found to be thermally stable at least up to 150°C. Optical studies reveal that the grown crystal has a maximum transmittance of 74% in the wavelength range 250 nm–1200 nm with the lower cut-off wavelength at 250 nm. From the mechanical study, it is understood that the BS crystal follows reverse indention size effect and belongs to soft material category. The electrical measurements indicate a normal dielectric behaviour and the electrical conduction could be explained as due to proton transport. In effect, the results of the present study indicate that the BS crystal grown by slow evaporation method is expected to be useful in photonic and sun screen devices.

5. REFERENCES

1. Srinivasan Natarajan, et al. (2012). The relevance of metal organic frameworks (MOFs) in inorganic materials chemistry. *J. Chem. Sci*., 124(2), 339–353. https://doi.org/10.1007/s12039-012-0239-z
2. Dhanya, V. S. et al. (2011). Growth and characterization of a new polymorph of lead succinate: A promising NLO material. *J. Cryst. Growth*, 319(1), 96–101. https://doi.org/10.1016/j.jcrysgro.2011.01.073
3. Binitha, M. P. & Pradyumnan, P. P. (2013). Structural, thermal and electrical characterization on gel grown copper succinate dihydrate single crystals. *Phys. Scr.*, 87(6), 065603. https://doi.org/10.1088/0031-8949/87/06/065603
4. Binitha, M. P. & Pradyumnan, P. P. (2014). Growth, characterization and dielectric property studies of gel grown barium succinate single crystals. *Bull. Mater. Sci.*, 37(3), 491–495. https://doi.org/10.1007/s12034-014-0662-5

5. Binitha, M. P. & Pradyumnan, P. P. (2014). Spectroscopic and dielectric studies of strontium succinate crystals. *Ind. J. Phys.*, 88(5), 497–500. https://doi.org/10.1007/s12648-014-0442-5
6. Pan, J. et al. (2007). Growth and characterization of a novel nonlinear optical crystal zinc succinate, Zn (C4H4O4). *J. Cryst. Growth*., 308(1), 89–92. https://doi.org/10.1016/j.jcrysgro.2007.05.057
7. Binitha, M. P. & Pradyumnan, P. P. (2014). Studies on growth, thermal and dielectric behavior of calcium succinate trihydrate single crystals. *J. Cryst. Growth*., 396, 38–44. https://doi.org/10.1016/j.jcrysgro.2014.03.033
8. Thayanithi, V. et al. (2017). Investigation of unidirectional growth and characterization of nonlinear optical L-alaninium p-toluenesulfonate crystal. *Mater. Res. Express*, 4(8), 086201. https://doi.org/10.1088/2053-1591/aa8080
9. Kurtz, S. K. & Perry, T. T. (1968). A powder technique for the evaluation of nonlinear optical materials. *J. Appl. Phys.* 39, 3798–3813. https://doi.org/10.1063/1.1656857
10. Vizhi, R. E. et al. (2015). Influence of sodium formate in γ-glycine single crystals–synthesis, growth and characterization. *Optik*, 126(1), 77–80. https://doi.org/10.1016/j.ijleo.2014.08.151
11. Vijila Manonmoni, J. et al. (2015). Synthesis, growth, structure and characterization of potassium lithium hydrogen phthalate mixed crystals. *RSC Adv.*, 5(57), 46282–46289. https://doi.org/10.1039/C5RA05634A
12. Amuthambigai, C. et al. (2016). Growth and characterization of bimetallic (Na and K) phthalate single crystals. *Appl. Phys. A*, 122(10), 1–8. https://doi.org/10.1007/s00339-016-0431-y
13. Wang, Y. U. et al. (2002). Phase field microelasticity theory and simulation of multiple voids and cracks in single crystals and polycrystals under applied stress. *J. Appl. Phys.*, 91(10), 6435–6451. https://doi.org/10.1063/1.1471389
14. Aggarwal M. D. et al. (2003). Bulk crystal growth and characterization of semiorganic nonlinear optical materials. *J. Optoele. Adv. Mater.*, 5(3), 555–562.
15. Ganesh, V. et al. (2014). Indentation studies on< 1 0 0>,< 0 0 1> and< 1 0 1> face of ammonium dihydrogen phosphate (ADP) single crystals: A novel nonlinear optical material. *Optik*, 125(13), 3268–3271. https://doi.org/10.1016/j.ijleo.2013.12.046
16. Onitsch E. M. (1956). The present status of testing the hardness of materials. *Mikroskopie*, 95(15), 12–14.
17. Sun, Z. et al. (2011). Synthesis, growth and characterization of a third-order nonlinear optical crystal based on the borate ester with sodium supporting its structural framework. *New J. Chemistry*, 35(12), 2804–2810. https://doi.org/10.1039/C1NJ20420C
18. Manonmani, N. et al. (2008). Growth and studies of two new potassium compound crystals. *Mater. Manuf. Processes.*, 23(2), 151–157. https://doi.org/10.1080/10426910701774619

19. Shkir, M. et al. (2013). Analysis on structural, SHG efficiency, optical and mechanical properties of KDP single crystals influenced by glycine doping. *Spectrochim. Acta A Mol. Biomol*., 103, 99–204. https://doi.org/10.1016/j.saa.2012.10.061
20. Christy, D. S. et al. (2017). Growth by free evaporation method and physico-chemical properties of calcium succinate single crystals. *Optik*, 145, 418–427. https://doi.org/10.1016/j.ijleo.2017.07.065
21. Peter, A. C. et al. (2010). Thermal, optical, mechanical and electrical properties of a novel NLO active L-phenylalanine L-phenylalaninium perchlorate single crystals. *Phys. B: Condens. Matter.*, 405(1), 65–71. https://doi.org/10.1016/j.physb.2009.08.035
22. Premkumar, P. S. (2020). Structural and Electrical Studies on Zinc Added Magnesium Oxide Nanoparticles. *J. Phys. Sci*, 31(3), 73–86. https://doi.org/10.21315/jps2020.31.3.6
23. Nadar J. S. J. et al. (2021). Studies on the physical properties of green synthesized cerium oxide nanoparticles using Melia Dubia leaf extract. *Mater. Today*. *Proc*., forthcoming. https://doi.org/10.1016/j.matpr.2021.10.035